

Draft genomes of three northern hemisphere blue mussel lineages: North and South European *Mytilus edulis* and Mediterranean *Mytilus galloprovincialis*.

Alexis Simon^{1,2,*}

¹ISEM, EPHE, IRD, Université Montpellier, Montpellier, France

²Center of Population Biology and Department of Evolution and Ecology, University of California Davis, Davis, California, USA

August 30, 2022

Abstract

The blue mussel species complex (*Mytilus edulis*) is of particular interest both as model species in population genetics and ecology, but also as an economic resource in many regions. Using 10X genomics pseudo long reads, I assembled genomes of closely related blue mussel lineages from the *Mytilus* species complex in the Northern hemisphere. Given the huge diversity within and between lineages in this complex, the objective was to produce affordable genomic resources for population and evolutionary genomic studies to broaden the coverage of this diverse species complex. I used transcriptome guided corrections and scaffolding on a chromosome scale genome of a close species to reduce the fragmentation of the genomes. The result is a set of partially fragmented genomes of equivalent completeness to already published genomes. Three new draft genomes are added to the fast increasing genomic resources of this complex for the Mediterranean *M. galloprovincialis*, the South-European *M. edulis* and the North-European *M. edulis*.

Keywords: *Mytilus edulis*, *Mytilus galloprovincialis*, Genome assembly, 10X chromium

* **Corresponding author:** alexis.simon@normalesup.org

1 Rationale and objectives

The *Mytilus* species complex has been a model system in population genetics, adaptation, hybridization and speciation since genetic variants could be identified (Ahmad et al., 1977; Bierne et al., 2003; Fraïsse et al., 2016; Koehn & Mitton, 1972; Milkman & Beaty, 1970; Quesada, Wenne, et al., 1995; Simon et al., 2021; Skibinski et al., 1978). This genus is also an important food source worldwide. While *Mytilus* species are actively cultured, human selection has been limited in blue mussels as most of the production rely on naturally captured spat. Therefore, given the extreme diversity observed within and between species in this genus, extensive genomic resources are needed to both advance our fundamental knowledge and potentially accrue our capacity to improve its culture in the face of large environmental changes.

The *Mytilus* species complex is composed of three taxonomically recognized and partially reproductively isolated species in the northern hemisphere, *Mytilus edulis*, *M. galloprovincialis* and *M. trossulus*; and several other species in the southern hemisphere (*M. chilensis*, *M. platensis*, *M. planulatus*). Between those species, hybridization is possible in contact zones, either natural or anthropogenic. Within each species, evolutionary relevant lineages can be identified: two lineages in *M. galloprovincialis*, (i) an Atlantic lineage (MgalATL) and (ii) a Mediterranean lineage (MgalMED), separated by a hybrid zone at the Almeria-Oran front and Algerian coast (El Ayari et al., 2019; Fraïsse et al., 2016; Quesada, Zapata, et al., 1995), and three lineages in *M. edulis*, (i) an American lineage (MeduAM), (ii) a Southern European lineage (MeduEUS), and (iii) a Northern European lineage (MeduEUN) (Fraïsse et al., 2016; Simon et al., 2020). Two close species in the genus are of interest: *M. coruscus*, a species found in Asia, and *M. californianus*, a species found on the Pacific coast of North America. While they do not appear to readily hybridize with species of the *Mytilus* species complex, they are of similar interest to the study of marine mussels.

Increased effort has been put in the last few years to produce genomic resources in the *Mytilus* species complex. Quality genomes are available for the following lineages of *Mytilus*: Atlantic *M. galloprovincialis* (Gerdol et al., 2020), Southern European *M. edulis* (Corrochano-Fraile et al., 2022), *M. coruscus* (R. Li et al., 2020; Yang et al., 2021), *M. californianus* (Paggeot et al., 2022), and an American *M. edulis* assembly (unpublished, accession GCA_019925275). This increased effort has highlighted characteristics of interest in those species such as a high proportion of gene presence-absence (Gerdol et al., 2020) or evidence of genome duplication (Corrochano-Fraile et al., 2022).

As an effort to diversify the genomic resources available for the *Mytilus* species complex, I assembled and annotated the genomes of three lineages using the 10X chromium technology. While these assemblies were initially fragmented due to the high level of heterozygosity, I leveraged the existence of a chromosome scale assembly of a sister species to scaffold against it. I obtained assemblies equivalent to published ones in term of completeness for three new lineages of the *Mytilus* species complex using a low sequencing budget and publicly available data. The resources produced and the assembly pipeline are freely available for use by the community.

2 Methods

General notes: The entire assembly was carried out using a Snakemake (Mölder et al., 2021) pipeline available on github at https://github.com/alxsimon/assembly_10x. Where

deemed important, parameters are given in the text. For brevity and simplicity, not all information might be available in the text. However, all parameters, software versions and steps are retrievable from the repository.

Important caveat: The assembled genome of MeduEUN (*M. edulis* Northern lineage) was initially thought to be *M. trossulus*. Therefore some assembly and annotation steps wrongly used *M. trossulus* transcriptomes. While this is not ideal, I think results have not been strongly impacted by this issue.

2.1 Biological material and DNA extraction

One individual for each species of interest was collected and processed fresh.

Collection locations:

- *M. galloprovincialis* Mediterranean (MgalMED); Sète (43°24'35.3"N, 3°41'41.1"E, Occitanie, France, Mediterranean Sea)
- *M. edulis* Southern European (MeduEUS); Agon-Coutainville (49°0'44.784"N, 1°35'55.643"W, Normandy, France, English Channel)
- *M. edulis* Northern Europe (MeduEUN); Mishukovo (69°02'34.3"N, 33°01'45.9"E, Kola Bay, Russia, Barents Sea)

Whole mussels were placed in 50 mL falcon tubes containing 25 ml of TNES-Urea solution and incubated for 4–6 weeks at room temperature (TNES-Urea: 10 mM Tris-HCl pH 7.4; 120 mM NaCl; 10 mM EDTA pH 8.0; 0.5% SDS; 4 M urea).

After this period of pre-treatment at ambient temperature, proteinase K was added at a final concentration of 150 µg/mL and the solution was incubated overnight at 56°C.

High Molecular weight genomic DNA was extracted following Nakayama et al. (1994). A 15 mL Phase Lock Gel Heavy extraction was used with three steps of extraction using phenol/chloroform/isoamyl alcohol (25/24/1 proportions) equilibrated with Tris-HCl to pH 8.1, followed by two chloroform extractions. After the last extraction, the aqueous supernatant was precipitated with 2 volumes of 100% EtOH and the pellet was hooked from the solution with a sterile glass Pasteur pipette. The pellet was rinsed several times with 80% EtOH before being dried at room temperature.

DNA was resuspended with an appropriate volume of biomolecular water at 65°C for several hours, the duration of this incubation depending on the size of the granules. DNA was then stored at 4°C.

Prior to the construction of the DNA libraries, DNA was repaired with NEBNext FFPE DNA Repair Mix according to the manufacturer's instructions.

2.2 Library preparation and sequencing

The 10X chromium library preparation and sequencing was subcontracted to the MGX platform (Montpellier, France). The 10X linked reads libraries for each individual were produced following the 10X Genomics Genome Reagen Kit (*Genome Solution*) protocol using a Chromium microfluidic chip. Libraries were subsequently sequenced on an Illumina NovaSeq 6000 with an S4 flowcell.

2.3 Preprocessing 10X reads

I preprocessed 10X reads using the following pipeline for use in several algorithms (section 2.4). I first removed duplicate reads using Nubeam-dedup (Dai and Guan, 2020; commit 25dd385). I then used proc10xG (<https://github.com/ucdavis-bioinformatics/proc10xG>; commit 7afbfcf) to split the reads from their 10X barcodes for further processing. I used a custom filtering step designed to remove under- and over-represented barcodes and their associated reads from the data (figs. S1 to S3, `filter_barcodes.R` script, personal communication of P-A Gagnaire). Reads were additionally filtered with fastp (v0.20.1; Chen et al., 2018) with the main objective to remove poly-G tails created by the Illumina Novaseq sequencing technology. I obtained at this point reads equivalent to a short-read sequencing run, usable in some parts of the assembly and quality control pipeline. Additionally, to obtain reads compatible to 10X genomics tools, I filtered and reassembled reads with their 10X barcodes in proc10xG using the `filter_10xReads.py` and `regen_10xReads.py` scripts.

2.4 Initial genome assemblies

For each genome I used Supernova v2.1.1 (Weisenfeld et al., 2017) to assemble raw 10X reads. To avoid hard stops in Supernova due to both data quantity slightly under 10X genomics recommendations and an overestimation of genome size by Supernova, I used all available reads (`--maxreads='all'`) and accepted extreme coverage (`--accept-extreme-coverage`). I produced every style of Fasta output available in Supernova but only used the pseudo-haploid output in the following pipeline.

To remove duplicate haplotypes in the assemblies, I followed the `purge_dups` pipeline (Guan et al., 2020; commit e1934bb). I first used the `longranger` v2.2.2 align algorithm to map preprocessed reads (section 2.3) to the pseudo-haploid genomes to use in the `ngscstat` step. `Minimap2` (v2.17; H. Li, 2017) was used in the contig self-mapping step. I obtained the purged assemblies using the `get_seqs` steps without restricting the purging to the end of contigs (without the `-e` option).

I used AGOUTI (<https://github.com/svm-zhang/AGOUTI>; commit a7e65d6; Zhang et al., 2016) to improve scaffolding by using paired end RNA-seq reads. For each species, a different set of published transcriptomes were used (see Supplementary File 1 for accession numbers). AGOUTI require a gene prediction as input in addition to RNA-seq reads. I used Augustus (v3.3.3; Stanke et al., 2008) to produce an intermediate annotation for each assembly using the *Caenorhabditis* model. RNA-seq reads were first cleaned using `rcorrector` (v1.0.4; Song and Florea, 2015) and `trimgalore` (v0.6.6; https://www.bioinformatics.babraham.ac.uk/projects/trim_galore; `--quality 20 --stringency 1 -e 0.1 --length 70`). RNA-seq reads were mapped independently using `bwa-mem2` (v2.2.1; Vasimuddin Md et al., 2019), and then merged as a common bam file for each assembly with `samtools` (v1.12; H. Li et al., 2009). Finally, the AGOUTI scaffolding pipeline was run using the gene prediction and mapped RNA-seq reads (`-minMQ 20 -maxFracMM 0.05`; using python v2.7.15 and `samtools` v1.10 for compatibility).

As a last step, I ran Blobtoolkit (v2.4.0; Challis et al., 2020) on the three assemblies to evaluate quality and potential contamination levels. I used a custom script (`btk_conta_extraction.py`) to filter the assembly contigs based on the taxids found by the Blobtoolkit pipeline to remove the most obvious contaminations. Contigs matching taxids associated with viruses, bacteria and non-mollusca eukaryotes were removed. More specifically contigs were removed for virus contamination if they presented a hit percentage of more than 10 % of their

length. Contigs were removed for eukaryote contamination only when presenting only hits to taxa outside Mollusca on more than 10 % of their length. The list of retained contigs was used to filter the fasta assembly file using seqkit (v0.13.2; Shen et al., 2016).

2.5 Scaffolding on the *Mytilus coruscus* genome

At the time of assembly, the closest relative of the *Mytilus* species of interest with a chromosome scale assembly was *Mytilus coruscus* (GCA_017311375.1; Yang et al., 2021). Given the conserved number of 14 chromosomes in the *Mytilus* genus, I decided to scaffold our contigs on this high quality reference. Additionally, I had Oxford Nanopore reads for the MeduEUN individual. I used minimap2 (v2.17; H. Li, 2017) and LRScf (v1.1.10; <https://github.com/shingocat/lrscaf>) to first improve the MeduEUN assembly with this small amount of long reads.

Then for each assembly, I ran the scaffolder RagTag (v1.1.1; Alonge et al., 2021) to position contigs on the *M. coruscus* chromosomal assembly.

A final polishing step was performed using Pilon (v1.24; Walker et al., 2014). Pilon attempts to improve the assembly based on mapped read information (gap filling and error corrections). I used bwa-mem2 to map the debarcoded and filtered 10X reads (section 2.3). In addition, Oxford Nanopore reads for MeduEUN were also used in Pilon for the given assembly.

2.6 Repeats

I masked repeats for the purpose of annotation using RepeatModeler (v2.0.1; Flynn et al., 2020) and RepeatMasker (v4.1.2-p1; Smit et al., 2013–2015) through the TETools DFAM container (v1.3.1; <https://hub.docker.com/r/dfam/tetools>). I first built repeat databases for each of five assemblies MgalMED, MeduEUS, MeduEUN, *M. coruscus* (GCA_017311375.1; Yang et al., 2021) and *M. galloprovincialis* from the Atlantic (GCA_900618805.1; Gerdol et al., 2020). Then, I built a common *Mytilus* database of repeats by merging those five databases using cd-hit (v4.8.1; Fu et al., 2012). I used the same options as used by default in RepeatModeler: -aS 0.8 -c 0.8 -g 1 -G 0 -A 80 -M 10000. Finally, soft repeat masking was performed on the assemblies with RepeatMasker using the merged database.

2.7 Annotation

I used Braker2 (v2.1.6; Brna et al., 2021) as to obtain structural annotations, using both a protein database and RNA-seq reads (preprocessed in section 2.4). To build the protein database, I used all *Mollusca* proteins (taxid 6447) from OrthoDB (v10.1; Kriventseva et al., 2019). To provide gene presence hints, I mapped all RNA-seq reads for each species using HISAT2 (v2.2.1; Kim et al., 2019).

I used the Mantis pipeline (v1.5.5; Queirós et al., 2021) to obtain consensus functional annotations of genes based on multiple databases. Protein sequences for each assembly were built from the structural annotations using the python module gff3tool (v2). Mantis was run with default parameters and databases: kofam (Aramaki et al., 2020), NPfM (Lu et al., 2020), eggNOG (Huerta-Cepas et al., 2019), pfam (EL-Gebali et al., 2019), and tcdb (Saier et al., 2021).

2.8 NCBI submission

The NCBI submission process identified a few errors that needed correction. A small number of adaptor sequences and duplicates were removed to comply with NCBI requirements (see the rule `ncbi_submission_changes.smk` in the pipeline for more details). Assemblies are available under the following accessions: JAKGDF000000000 for MgalMED, JAKGDG000000000 for MeduEUS, and JAKGDH000000000 for MeduEUN.

2.9 Quality assessments and comparisons

Preprocessed 10X reads (section 2.3) were used to first estimate genome size and heterozygosities of the three individuals. I used the reference free k-mer based method GenomeScope (<https://github.com/tbenavi1/genomescope2.0>; commit 5034ed4; Ranallo-Benavidez et al., 2020) and the fork of the KMC k-mer counting program (<https://github.com/tbenavi1/KMC>; commit 1df71f6).

Assembly statistics were computed with the python module `assembly_stats` (v0.1.4; Trizna, 2020).

To assess the remaining level of duplication in the assemblies, I used the program KAT (v2.4.2; Mapleson et al., 2017) to compare k-mer spectra from reads (preprocessed 10X) and from the assembly.

Finally, gene completion analyses were carried out using BUSCO (v5.1.1; Manni et al., 2021). I used both a Metazoan (`metazoa_odb10.2021-02-24`) and Molluscan (`mollusca_odb10.2020-08-05`) database to assess and compare new and published assemblies. I compared our assemblies to the following published ones:

- *M. coruscus*, GCA_017311375.1, Yang et al. (2021);
- *M. galloprovincialis* from the Atlantic lineage, GCA_900618805.1, Gerdol et al. (2020);
- *M. edulis* from the Southern European lineage, GCA_905397895.1, Corrochano-Fraile et al. (2022)
- *M. edulis* from the American lineage, GCA_019925275.1.

2.10 Phylogenetic species tree

I compiled protein sequences from published *Mytilus* genomes and transcriptomes, in addition to the current three genomes and annotations, to build a species tree. I used transcriptomes produced in Popovic and Riginos (2020) for American *M. edulis*, Mediterranean *M. galloprovincialis*, *M. trossulus*, *M. californianus*. Transcriptomes were translated using the `seqkit` program (v2.2.0; Shen et al., 2016) I used genomes and associated annotations of *M. coruscus* (GCA_017311375.1; Yang et al., 2021), Southern European *M. edulis* (GCA_905397895.1; Corrochano-Fraile et al., 2022), Atlantic *M. galloprovincialis* (GCA_900618805.1; Gerdol et al., 2020), and American *M. edulis* (GCA_019925275.1; annotation as personal communication of Tiago Hori, PEIMSO). For GCA_019925275.1, protein sequences were retrieved from the fasta and gff files using the python module `gff3tool` (v2.1.0).

I used OrthoFinder (v2.5.4; Emms and Kelly, 2015, 2019) to find orthogroups and orthologue genes. Species tree was inferred using the MSA method of OrthoFinder (Emms

& Kelly, 2018) using the MAFFT aligner (v7.505; Katoh and Standley, 2013), the STRIDE species tree rooting algorithm (Emms & Kelly, 2017) and the FastTree software for tree inference (v2.1.11; Price et al., 2009).

3 Results and discussion

3.1 Assembly results

I introduce here newly assembled genomes from three lineages of the *Mytilus* species complex. With a limited sequencing budget of ~ 3000 per genome, I managed to produce draft genomes of enough quality to be useful in applications such as population genomics and genetics. The method of 10X chromium pseudo-long reads combined with scaffolding using published data provided a quality comparable to published assemblies for *Mytilus* species.

The pre-assembly k-mer analysis carried out using GenomeScope (using 21-mers) showed that, as expected, the genomes of MgalMED and MeduEUN were highly heterozygous with values of 3.49 and 4.03 % respectively (fig. 1). The heterozygous peak of MeduEUS was not identifiable due to lower sequencing depth and GenomeScope provides a bad quality fit that I did not interpret.

Highly heterozygous genomes brings the risk of having a large number of duplicate contigs due to the separate assembly of the multiple alleles from given locus. For this reason, I used the `purge_dups` pipeline to try removing a maximum of such bias. This procedure reduced the number of complete duplicated genes in all assemblies (fig. S5, v1 to v4). Overall, the compared KAT spectra analyses show that the assembly steps reduced the amount of duplication in all assemblies (fig. S4).

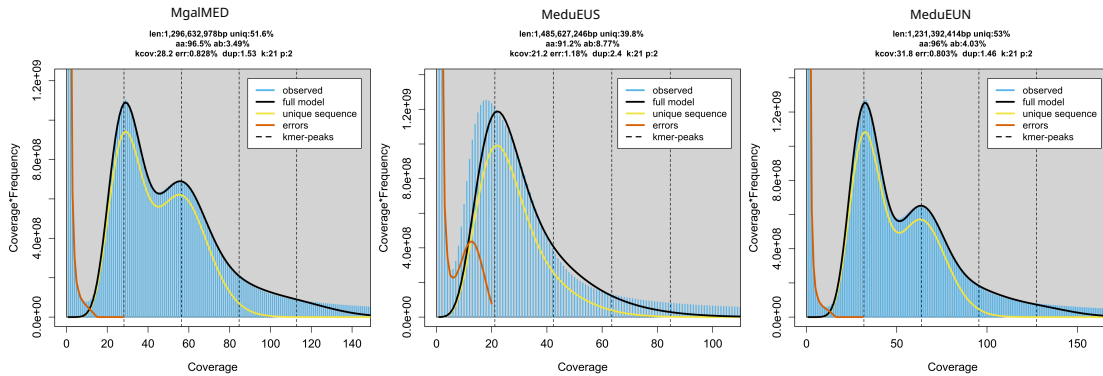


Figure 1: k-mer profile plots computed with 21-mers using GenomeScope. Coverage histogram of the k-mers in blue. Lines represent the fit of the GenomeScope models. len: inferred genome length; uniq: percentage of the genome that is unique, aa: overall homozygosity; ab: overall heterozygosity; kcov: mean k-mer coverage for heterozygous bases; err: reads error rate; dup: average rate of read duplication; k: k-mer size; p: ploidy.

Assembly statistics for the three new assemblies and four publicly available assemblies are presented in table 1 (complete statistics are presented in Supplementary File 2). With the exception of MeduEUS, GC content and genome sizes are close to what is found in other lineages. While the number of scaffolds for the new assemblies is still high, most of the genomes are contained in 14 large scaffolds corresponding to the number of chromosomes

found in *Mytilus* species. Residual scaffolds are sequences that could not be placed on the *M. coruscus* genome, maybe due to inter-species presence-absence or too high divergence.

Table 1: Assembly statistics comparisons. C for contigs and S for scaffolds.

assembly	C.L50	C.N50	C.median	C.sequence_count	S.L50	S.N50	S.gc_content	S.median	S.sequence_count	S.total_bps
Mcor_GCA017311375	2.61×10^2	1.48×10^6	4.21×10^4	6449	6	9.95×10^7	32.4	2.13×10^4	4434	1.57×10^9
MgalATL_GCA900618805	4.92×10^3	7.70×10^4	3.95×10^4	22922	1903	2.08×10^5	32.1	7.76×10^4	10577	1.28×10^9
MeduEUS_GCA905397895	9.77×10^2	5.11×10^5	1.85×10^5	5966	464	1.10×10^6	32.2	2.92×10^5	3339	1.83×10^9
MeduAM_GCA019925415	8.35×10^2	4.91×10^5	6.25×10^4	9686	6	1.17×10^8	32.3	2.89×10^4	1119	1.65×10^9
MgalMED_v7	1.69×10^4	2.63×10^4	7.48×10^3	115913	9	7.20×10^7	32.1	4.53×10^3	41122	1.66×10^9
MeduEUS_v7	2.45×10^4	2.36×10^4	6.48×10^3	169324	415	2.28×10^5	34.6	5.00×10^3	73616	2.08×10^9
MeduEUN_v7	1.59×10^4	2.92×10^4	8.96×10^3	105892	9	7.71×10^7	32.1	6.16×10^3	28220	1.76×10^9

To assess the completeness of our assemblies, I compared them to four *Mytilus* published assemblies on the basis of a Metazoan and a Molluscan set of single copy orthologous genes using BUSCO (fig. 2). Overall, I show that our assemblies are equivalent to the published ones in terms of completeness.

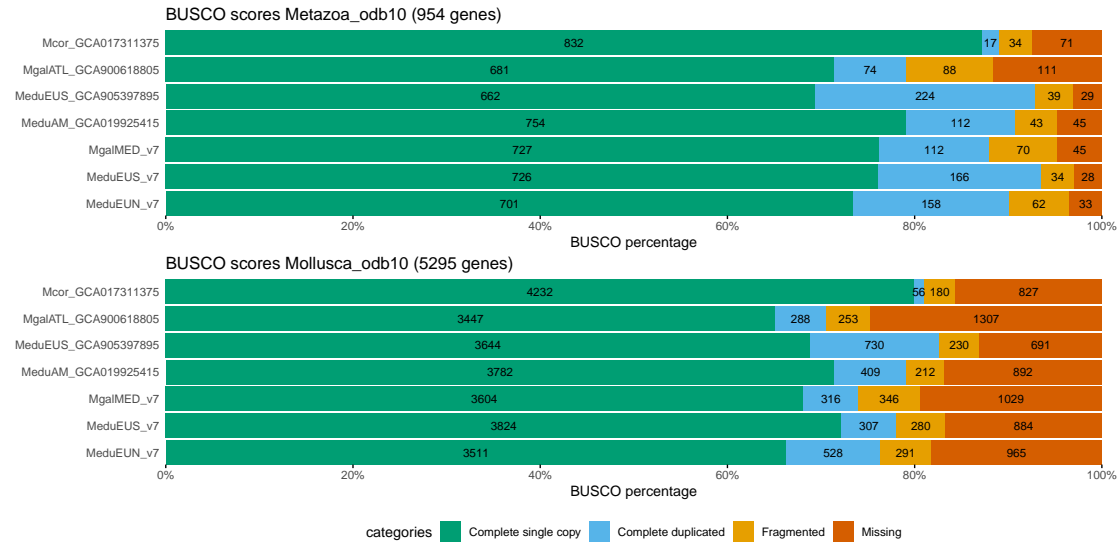


Figure 2: Busco scores

The MeduEUS assembly suffered from an increased level of contamination compared to the other two assemblies. Despite a broad contaminant filtering step, the Busco blob analysis (fig. S7) shows a second GC content peak centered around 40% (above the 32% peaks of this and other genomes). This contamination could for instance be due to bacteria present in the mussel if its physiological state was degraded before fixation. The metagenomic composition of contaminants was not investigated.

3.2 Repeat contents

More than half of each genome was identified as repeats and masked by RepeatMasker. Repeats are estimated to amount to 57.22, 61.10 and 55.53% of MgalMED, MeduEUS and MeduEUN assemblies respectively. The majority of repeats are unclassified, followed by retroelements with a balanced contribution of LINES and LTR elements (detailed RepeatMasker results in table S2).

3.3 Annotations

The assemblies were annotated using a consensus pipeline to provide additional resources for future uses. These annotation were used to produce the following species tree.

3.4 Species tree

OrthoFinder assigned 499004 genes (91.9% of total) to 50543 orthogroups. Fifty percent of all genes were in orthogroups with 13 or more genes (G50 was 13) and were contained

in the largest 11982 orthogroups (O50 was 11982). There were 1852 orthogroups with all species present and 173 of these consisted entirely of single-copy genes.

The species tree was built using 1300 orthogroups with a minimum of 81.8% of species having single-copy genes in any orthogroup (fig. 3). It shows that the assemblies and the published genomes and transcriptomes are clustering as expected.

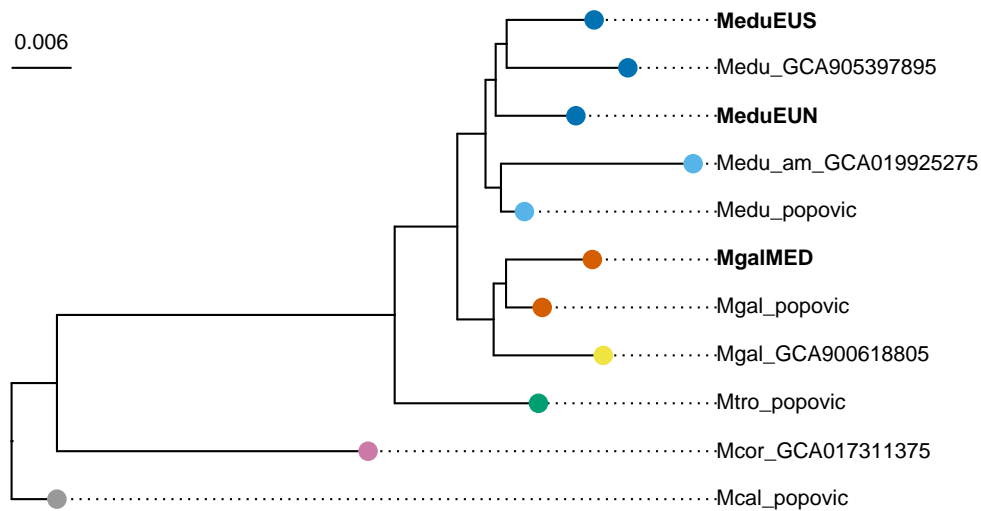


Figure 3: Species tree using 1300 orthogroups with a minimum of 81.8% of species having single-copy genes in any orthogroup. Color coding – dark blue: *M. edulis* Europe, light blue: *M. edulis* America, red: *M. galloprovincialis* Mediterranean Sea, yellow: *M. galloprovincialis* Atlantic, green: *M. trossulus*, pink: *M. coruscus*, gray: *M. californianus*.

Data availability

Raw data are available under BioProject PRJNA785550. Assemblies are available under accessions JAKGDF000000000 (MgalMED), JAKGDG000000000 (MeduEUS), and JAKGDH000000000 (MeduEUN). The assembly pipeline is available at https://github.com/alxsimon/assembly_10x. Annotations, and the OrthoFinder pipeline and results are available in the Zenodo archive 10.5281/zenodo.7034399. Data and code for this manuscript are available at https://github.com/alxsimon/Mytilus_ref_genomes_paper.

Acknowledgements

I thank Nicolas Bierne and Pierre-Alexandre Gagnaire for their help on the project and discussions; Christine Arbiol for DNA extractions; Maurine Hammel and Erika Burioli for sharing their transcriptome data; and Petr Strelkov for sampling of the *M. trossulus*. Some bioinformatic analyses were performed on the Core Cluster of the Institut Français de Bioinformatique (ANR-11-INBS-0013). I thank Tiago Horri for providing his annotation of the American *Mytilus edulis* genome (GCA.019925275.1). AS was supported by the French ANR grant TRANSCAN (ANR-18-CE35-0009) and by the National Institute of General

Medical Sciences of the National Institutes of Health (grants NIH R01 GM108779 and R35 GM136290 to Graham Coop).

References

- Ahmad, M., Skibinski, D. O. F., & Beardmore, J. A. (1977). An estimate of the amount of genetic variation in the common mussel *Mytilus edulis*. *Biochemical Genetics*, 15(9–10), 833–846. <https://doi.org/10.1007/BF00483980>
- Alonge, M., Lebeigle, L., Kirsche, M., Aganezov, S., Wang, X., Lippman, Z. B., Schatz, M. C., & Soyk, S. (2021). Automated assembly scaffolding elevates a new tomato system for high-throughput genome editing. *bioRxiv*, 2021.11.18.469135. <https://doi.org/10.1101/2021.11.18.469135>
- Aramaki, T., Blanc-Mathieu, R., Endo, H., Ohkubo, K., Kanehisa, M., Goto, S., & Ogata, H. (2020). KofamKOALA: KEGG Ortholog assignment based on profile HMM and adaptive score threshold. *Bioinformatics*, 36(7), 2251–2252. <https://doi.org/10.1093/bioinformatics/btz859>
- Bierne, N., Borsa, P., Daguin, C., Jollivet, D., Viard, F., Bonhomme, F., & David, P. (2003). Introgression patterns in the mosaic hybrid zone between *Mytilus edulis* and *M. galloprovincialis*. *Molecular Ecology*, 12(2), 447–461. <https://doi.org/10.1046/j.1365-294X.2003.01730.x>
- Brna, T., Hoff, K. J., Lomsadze, A., Stanke, M., & Borodovsky, M. (2021). BRAKER2: Automatic eukaryotic genome annotation with GeneMark-EP+ and AUGUSTUS supported by a protein database. *NAR Genomics and Bioinformatics*, 3(1), lqaa108. <https://doi.org/10.1093/nargab/lqaa108>
- Challis, R., Richards, E., Rajan, J., Cochrane, G., & Blaxter, M. (2020). BlobToolKit Interactive Quality Assessment of Genome Assemblies. *G3 Genes—Genomes—Genetics*, 10(4), 1361–1374. <https://doi.org/10.1534/g3.119.400908>
- Chen, S., Zhou, Y., Chen, Y., & Gu, J. (2018). Fastp: An ultra-fast all-in-one FASTQ preprocessor. *Bioinformatics*, 34, i884–i890. <https://doi.org/10.1093/bioinformatics/bty560>
- Corrochano-Fraile, A., Davie, A., Carboni, S., & Bekaert, M. (2022). Evidence of multiple genome duplication events in *Mytilus* evolution. *BMC Genomics*, 23(1), 340. <https://doi.org/10.1186/s12864-022-08575-9>
- Dai, H., & Guan, Y. (2020). Nubeam-dedup: A fast and RAM-efficient tool to de-duplicate sequencing reads without mapping (I. Birol, Ed.). *Bioinformatics*, 36(10), 3254–3256. <https://doi.org/10.1093/bioinformatics/btaa112>
- El Ayari, T., Trigui El Menif, N., Hamer, B., Cahill, A. E., & Bierne, N. (2019). The hidden side of a major marine biogeographic boundary: A wide mosaic hybrid zone at the AtlanticMediterranean divide reveals the complex interaction between natural and genetic barriers in mussels. *Heredity*, 122, 770–784. <https://doi.org/10.1038/s41437-018-0174-y>
- El-Gebali, S., Mistry, J., Bateman, A., Eddy, S. R., Luciani, A., Potter, S. C., Qureshi, M., Richardson, L. J., Salazar, G. A., Smart, A., Sonnhammer, E. L. L., Hirsh, L., Paladin, L., Piovesan, D., Tosatto, S. C. E., & Finn, R. D. (2019). The Pfam protein families database in 2019. *Nucleic Acids Research*, 47(D1), D427–D432. <https://doi.org/10.1093/nar/gky995>
- Emms, D. M., & Kelly, S. (2018). STAG: Species Tree Inference from All Genes. *bioRxiv*, 267914. <https://doi.org/10.1101/267914>

- Emms, D. M., & Kelly, S. (2015). OrthoFinder: Solving fundamental biases in whole genome comparisons dramatically improves orthogroup inference accuracy. *Genome Biology*, 16(1), 157. <https://doi.org/10.1186/s13059-015-0721-2>
- Emms, D. M., & Kelly, S. (2017). STRIDE: Species Tree Root Inference from Gene Duplication Events. *Molecular Biology and Evolution*, 34(12), 3267–3278. <https://doi.org/10.1093/molbev/msx259>
- Emms, D. M., & Kelly, S. (2019). OrthoFinder: Phylogenetic orthology inference for comparative genomics. *Genome Biology*, 20(1), 238. <https://doi.org/10.1186/s13059-019-1832-y>
- Flynn, J. M., Hubley, R., Goubert, C., Rosen, J., Clark, A. G., Feschotte, C., & Smit, A. F. (2020). RepeatModeler2 for automated genomic discovery of transposable element families. *Proceedings of the National Academy of Sciences*, 117(17), 9451–9457. <https://doi.org/10.1073/pnas.1921046117>
- Fraïsse, C., Belkhir, K., Welch, J. J., & Bierne, N. (2016). Local interspecies introgression is the main cause of extreme levels of intraspecific differentiation in mussels. *Molecular Ecology*, 25(1), 269–286. <https://doi.org/10.1111/mec.13299>
- Fu, L., Niu, B., Zhu, Z., Wu, S., & Li, W. (2012). CD-HIT: Accelerated for clustering the next-generation sequencing data. *Bioinformatics*, 28(23), 3150–3152. <https://doi.org/10.1093/bioinformatics/bts565>
- Gerdol, M., Moreira, R., Cruz, F., Gómez-Garrido, J., Vlasova, A., Rosani, U., Venier, P., Naranjo-Ortiz, M. A., Murgarella, M., Greco, S., Balseiro, P., Corvelo, A., Frias, L., Gut, M., Gabaldón, T., Pallavicini, A., Canchaya, C., Novoa, B., Alioto, T. S., ... Figueras, A. (2020). Massive gene presence-absence variation shapes an open pan-genome in the Mediterranean mussel. *Genome Biology*, 21(1), 275. <https://doi.org/10.1186/s13059-020-02180-3>
- Guan, D., McCarthy, S. A., Wood, J., Howe, K., Wang, Y., & Durbin, R. (2020). Identifying and removing haplotypic duplication in primary genome assemblies. *Bioinformatics*, 36(9), 2896–2898. <https://doi.org/10.1093/bioinformatics/btaa025>
- Huerta-Cepas, J., Szklarczyk, D., Heller, D., Hernández-Plaza, A., Forslund, S. K., Cook, H., Mende, D. R., Letunic, I., Rattei, T., Jensen, L. J., von Mering, C., & Bork, P. (2019). eggNOG 5.0: A hierarchical, functionally and phylogenetically annotated orthology resource based on 5090 organisms and 2502 viruses. *Nucleic Acids Research*, 47(D1), D309–D314. <https://doi.org/10.1093/nar/gky1085>
- Katoh, K., & Standley, D. M. (2013). MAFFT Multiple Sequence Alignment Software Version 7: Improvements in Performance and Usability. *Molecular Biology and Evolution*, 30(4), 772–780. <https://doi.org/10.1093/molbev/mst010>
- Kim, D., Paggi, J. M., Park, C., Bennett, C., & Salzberg, S. L. (2019). Graph-based genome alignment and genotyping with HISAT2 and HISAT-genotype. *Nature Biotechnology*, 37(8), 907–915. <https://doi.org/10.1038/s41587-019-0201-4>
- Koehn, R. K., & Mitton, J. B. (1972). Population Genetics of Marine Pelecypods. I. Ecological Heterogeneity and Evolutionary Strategy at an Enzyme Locus. *The American Naturalist*, 106(947), 47–56. <https://doi.org/10.1086/282750>
- Kriventseva, E. V., Kuznetsov, D., Tegenfeldt, F., Manni, M., Dias, R., Simão, F. A., & Zdobnov, E. M. (2019). OrthoDB v10: Sampling the diversity of animal, plant, fungal, protist, bacterial and viral genomes for evolutionary and functional annotations of orthologs. *Nucleic Acids Research*, 47(D1), D807–D811. <https://doi.org/10.1093/nar/gky1053>
- Li, H., Handsaker, B., Wysoker, A., Fennell, T., Ruan, J., Homer, N., Marth, G., Abecasis, G., Durbin, R., & 1000 Genome Project Data Processing Subgroup. (2009). The

- Sequence Alignment/Map format and SAMtools. *Bioinformatics*, 25(16), 2078–2079. <https://doi.org/10.1093/bioinformatics/btp352>
- Li, H. (2017). *Minimap2: Pairwise alignment for nucleotide sequences*.
- Li, R., Zhang, W., Lu, J., Zhang, Z., Mu, C., Song, W., Migaud, H., Wang, C., & Bekaert, M. (2020). The Whole-Genome Sequencing and Hybrid Assembly of *Mytilus coruscus*. *Frontiers in Genetics*, 11, 440. <https://doi.org/10.3389/fgene.2020.00440>
- Lu, S., Wang, J., Chitsaz, F., Derbyshire, M. K., Geer, R. C., Gonzales, N. R., Gwadz, M., Hurwitz, D. I., Marchler, G. H., Song, J. S., Thanki, N., Yamashita, R. A., Yang, M., Zhang, D., Zheng, C., Lanczycki, C. J., & Marchler-Bauer, A. (2020). CDD/SPARCLE: The conserved domain database in 2020. *Nucleic Acids Research*, 48(D1), D265–D268. <https://doi.org/10.1093/nar/gkz991>
- Manni, M., Berkeley, M. R., Seppey, M., Simão, F. A., & Zdobnov, E. M. (2021). BUSCO Update: Novel and Streamlined Workflows along with Broader and Deeper Phylogenetic Coverage for Scoring of Eukaryotic, Prokaryotic, and Viral Genomes. *Molecular Biology and Evolution*, 38(10), 4647–4654. <https://doi.org/10.1093/molbev/msab199>
- Mapleson, D., Garcia Accinelli, G., Kettleborough, G., Wright, J., & Clavijo, B. J. (2017). KAT: A K-mer analysis toolkit to quality control NGS datasets and genome assemblies. *Bioinformatics*, 33(4), 574–576. <https://doi.org/10.1093/bioinformatics/btw663>
- Milkman, R., & Beaty, L. (1970). Large-Scale Electrophoretic Studies of Allelic Variation in *Mytilus edulis*. *Biological Bulletin*, 139, 430.
- Mölder, F., Jablonski, K., Letcher, B., Hall, M., Tomkins-Tinch, C., Sochat, V., Forster, J., Lee, S., Twardziok, S., Kanitz, A., Wilm, A., Holtgrewe, M., Rahmann, S., Nahnsen, S., & Köster, J. (2021). Sustainable data analysis with Snakemake [version 2; peer review: 2 approved]. *F1000Research*, 10(33). <https://doi.org/10.12688/f1000research.29032.2>
- Nakayama, I., Foresti, F., Tewari, R., Schartl, M., & Chourrout, D. (1994). Sex chromosome polymorphism and heterogametic males revealed by two cloned DNA probes in the ZW/ZZ fish *Leporinus elongatus*. *Chromosoma*, 103(1), 31–39. <https://doi.org/10.1007/BF00364723>
- Paggeot, L. X., DeBiasse, M. B., Escalona, M., Fairbairn, C., Marimuthu, M. P. A., Nguyen, O., Sahasrabudhe, R., & Dawson, M. N. (2022). Reference genome for the California ribbed mussel, *Mytilus californianus*, an ecosystem engineer. *Journal of Heredity*, esac041. <https://doi.org/10.1093/jhered/esac041>
- Popovic, I., & Riginos, C. (2020). Comparative genomics reveals divergent thermal selection in warm and coldtolerant marine mussels. *Molecular Ecology*, 29(3), 519–535. <https://doi.org/10.1111/mec.15339>
- Price, M. N., Dehal, P. S., & Arkin, A. P. (2009). FastTree: Computing Large Minimum Evolution Trees with Profiles instead of a Distance Matrix. *Molecular Biology and Evolution*, 26(7), 1641–1650. <https://doi.org/10.1093/molbev/msp077>
- Queirós, P., Delogu, F., Hickl, O., May, P., & Wilmes, P. (2021). Mantis: Flexible and consensus-driven genome annotation. *GigaScience*, 10(6), giab042. <https://doi.org/10.1093/gigascience/giab042>
- Quesada, H., Wenne, R., & Skibinski, D. O. F. (1995). Differential introgression of mitochondrial DNA across species boundaries within the marine mussel genus *Mytilus*. *Proceedings of the Royal Society B: Biological Sciences*, 262(1363), 51–56. <https://doi.org/10.1098/rspb.1995.0175>
- Quesada, H., Zapata, C., & Alvarez, G. (1995). A multilocus allozyme discontinuity in the mussel *Mytilus galloprovincialis*: The interaction of ecological and life-history factors. *Marine Ecology Progress Series*, 116, 99–115.

- Ranallo-Benavidez, T. R., Jaron, K. S., & Schatz, M. C. (2020). GenomeScope 2.0 and Smudgeplot for reference-free profiling of polyploid genomes. *Nature Communications*, 11(1), 1432. <https://doi.org/10.1038/s41467-020-14998-3>
- Saier, M. H., Jr, Reddy, V. S., Moreno-Hagelsieb, G., Hendargo, K. J., Zhang, Y., Iddamsetty, V., Lam, K. J. K., Tian, N., Russum, S., Wang, J., & Medrano-Soto, A. (2021). The Transporter Classification Database (TCDB): 2021 update. *Nucleic Acids Research*, 49(D1), D461–D467. <https://doi.org/10.1093/nar/gkaa1004>
- Shen, W., Le, S., Li, Y., & Hu, F. (2016). SeqKit: A Cross-Platform and Ultrafast Toolkit for FASTA/Q File Manipulation (Q. Zou, Ed.). *PLOS ONE*, 11(10), e0163962. <https://doi.org/10.1371/journal.pone.0163962>
- Simon, A., Arbiol, C., Nielsen, E. E., Couteau, J., Sussarellu, R., Burgeot, T., Bernard, I., Coolen, J. W. P., Lamy, J.-B., Robert, S., Skazina, M., Strelkov, P., Queiroga, H., Cancio, I., Welch, J. J., Viard, F., & Bierne, N. (2020). Replicated anthropogenic hybridisations reveal parallel patterns of admixture in marine mussels. *Evolutionary Applications*, 13(3), 575–599. <https://doi.org/10.1111/eva.12879>
- Simon, A., Fraïsse, C., El Ayari, T., LiautardHaag, C., Strelkov, P., Welch, J. J., & Bierne, N. (2021). How do species barriers decay? Concordance and local introgression in mosaic hybrid zones of mussels. *Journal of Evolutionary Biology*, 34, 208–223. <https://doi.org/10.1111/jeb.13709>
- Skibinski, D. O. F., Ahmad, M., & Beardmore, J. A. (1978). Genetic evidence of naturally occurring hybrids between *Mytilus edulis* and *M. galloprovincialis*. 32(2), 354–364. <https://doi.org/10.1038/nature01240>
- Smit, A., Hubley, R., & Green, P. (2013–2015). *RepeatMasker Open-4.0* (Version 4.1.2-p1).
- Song, L., & Florea, L. (2015). Rcorrector: Efficient and accurate error correction for Illumina RNA-seq reads. *GigaScience*, 4(1), 48. <https://doi.org/10.1186/s13742-015-0089-y>
- Stanke, M., Diekhans, M., Baertsch, R., & Haussler, D. (2008). Using native and syntenically mapped cDNA alignments to improve de novo gene finding. *Bioinformatics*, 24(5), 637–644. <https://doi.org/10.1093/bioinformatics/btn013>
- Trizna, M. (2020). *Assembly_stats 0.1.4* (Version 0.1.4). <https://doi.org/10.5281/zenodo.3968775>
- Vasimuddin Md, S. M., Misra, S., Li, H., & Aluru, S. (2019). *Efficient Architecture-Aware Acceleration of BWA-MEM for Multicore Systems*.
- Walker, B. J., Abeel, T., Shea, T., Priest, M., Abouelliel, A., Sakthikumar, S., Cuomo, C. A., Zeng, Q., Wortman, J., Young, S. K., & Earl, A. M. (2014). Pilon: An Integrated Tool for Comprehensive Microbial Variant Detection and Genome Assembly Improvement. *PLOS ONE*, 9(11), 14.
- Weisenfeld, N. I., Kumar, V., Shah, P., Church, D. M., & Jaffe, D. B. (2017). Direct determination of diploid genome sequences. *Genome Research*, 27(5), 757–767. <https://doi.org/10.1101/gr.214874.116>
- Yang, J.-L., Feng, D.-D., Liu, J., Xu, J.-K., Chen, K., Li, Y.-F., Zhu, Y.-T., Liang, X., & Lu, Y. (2021). Chromosome-level genome assembly of the hard-shelled mussel *Mytilus coruscus*, a widely distributed species from the temperate areas of East Asia. *GigaScience*, 10. <https://doi.org/10.1093/gigascience/giab024>
- Zhang, S. V., Zhuo, L., & Hahn, M. W. (2016). AGOUTI: Improving genome assembly and annotation using transcriptome data. *GigaScience*, 5(1), 31. <https://doi.org/10.1186/s13742-016-0136-3>

Supplementary Information

Tables

Table S1: Steps carried out for each version of assembly

Version	Step	
v1	Raw assembly from Supernova	
v2	Supernova assembly using a filtered dataset of reads (section 2.3)	
v3	Assembly with purged duplicates (<code>purge_dups</code>) from v3	Unused
v4	Assembly with purged duplicates (<code>purge_dups</code>) from v1	
v5	Agouti repaired scaffolds from v4	
v6	Assembly with filtered contamination using Blobtoolkit results	
v7	Scaffolded assembly on <i>M. coruscus</i>	

Figures

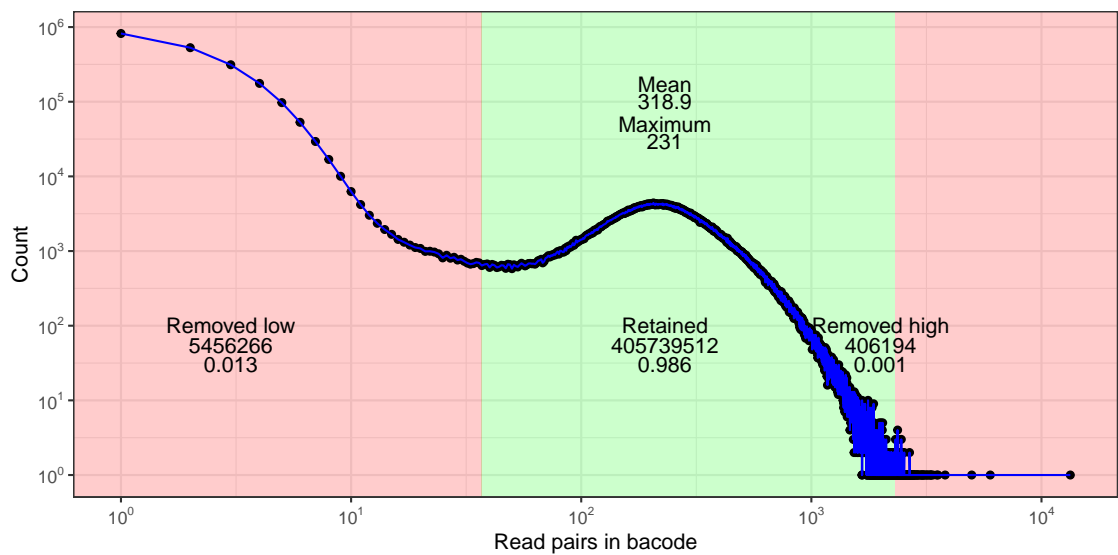


Figure S1: Histogram of read pairs identified for each 10X barcode for MgalMED. As part of preprocessing step, barcodes for which too few or too many read pairs are associated with each unique barcode are removed from the dataset (red regions).

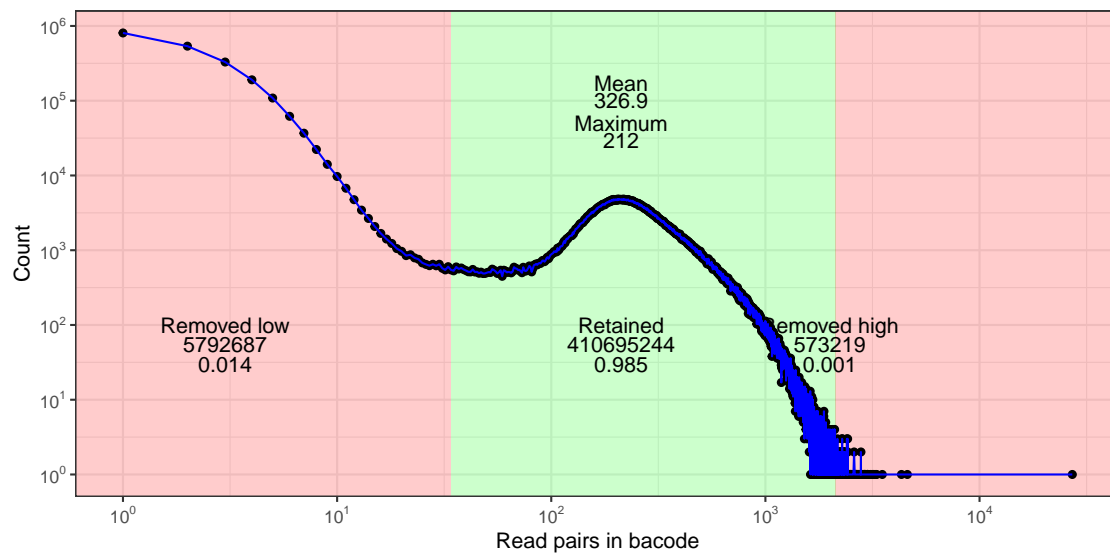


Figure S2: Histogram of read pairs identified for each 10X barcode for MeduEUS. As part of preprocessing step, barcodes for which too few or too many read pairs are associated with each unique barcode are removed from the dataset (red regions).

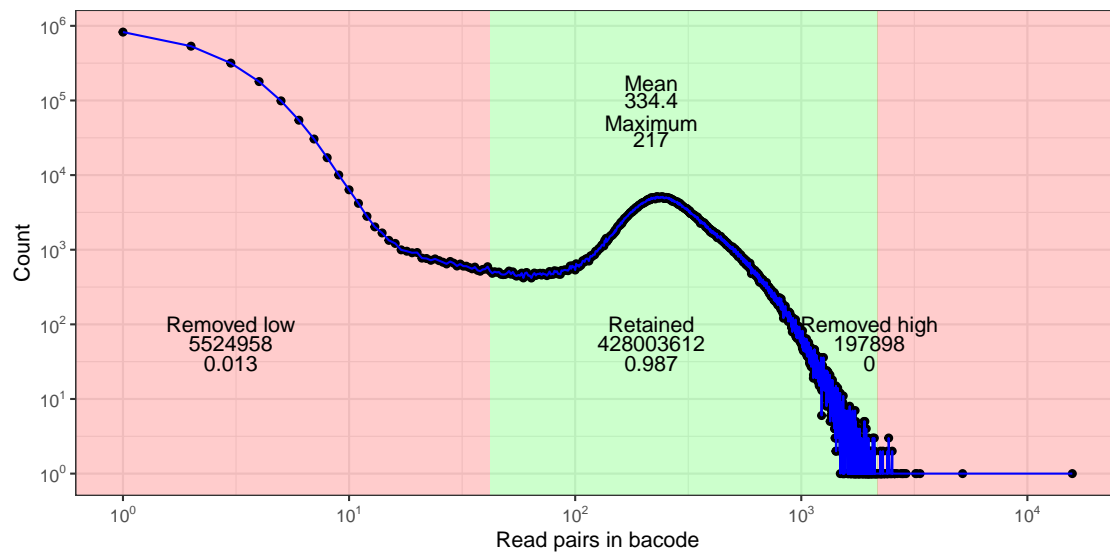


Figure S3: Histogram of read pairs identified for each 10X barcode for MeduEUN. As part of preprocessing step, barcodes for which too few or too many read pairs are associated with each unique barcode are removed from the dataset (red regions).

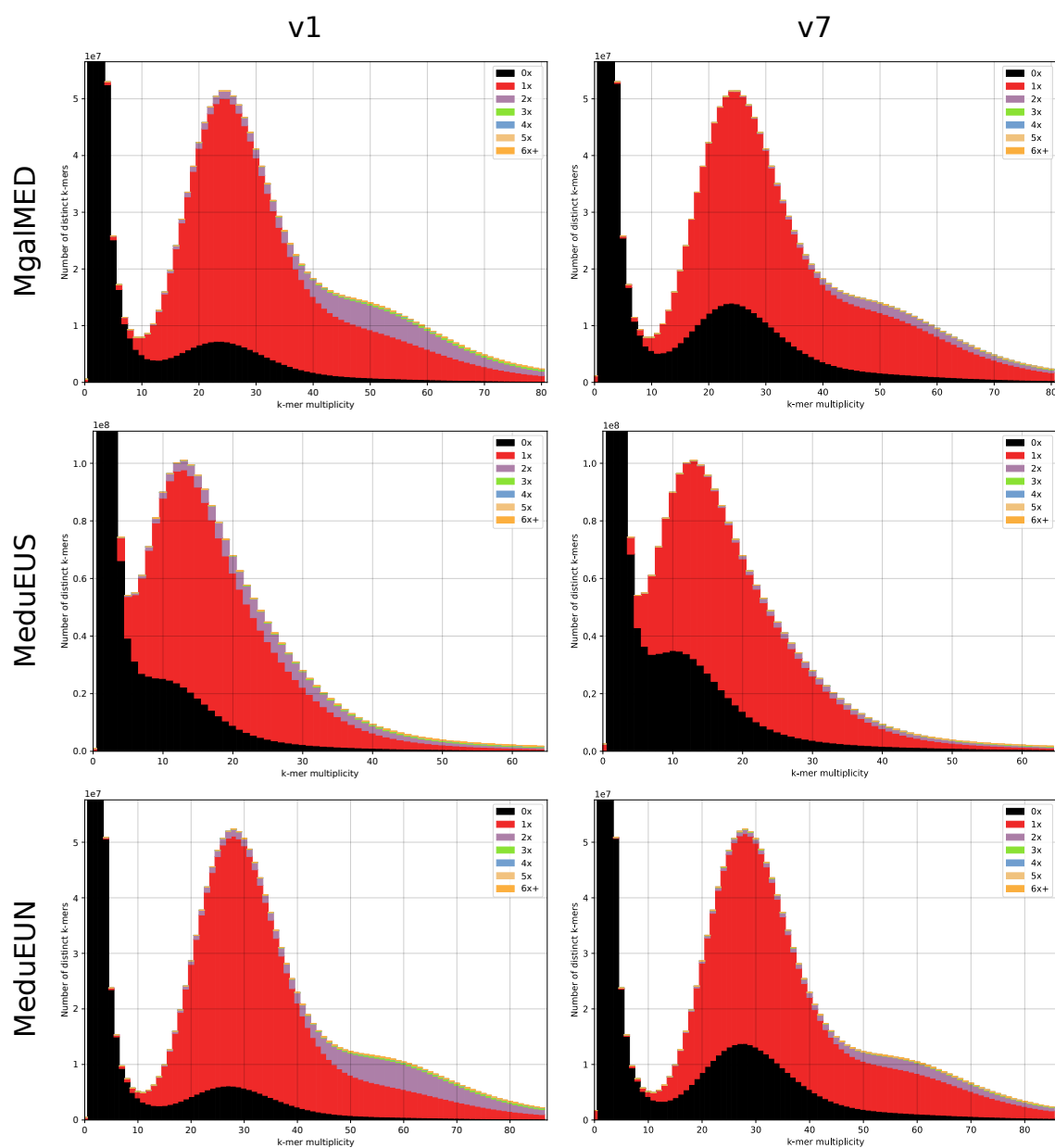


Figure S4: KAT comparison of k-mer spectra between assembly and preprocessed reads. Results are compared between the initial assembly (v1, left column) and the final assembly (v7, right column) for each sample MgalMED, MeduEUS and MeduEUN (from top to bottom).

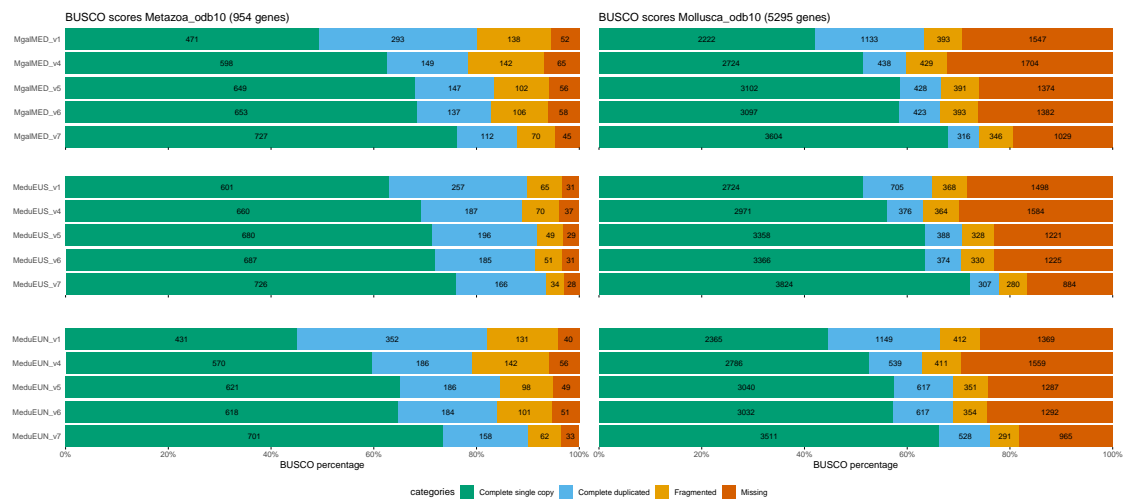


Figure S5: Busco scores on the metazoa_odb10 (left panels) and mollusca_odb10 (right panels) databases for each assembly MgalMED, MeduEUS and MeduEUN (top to bottom panels) across several assembly versions (v1, v4, v5, v6, v7).

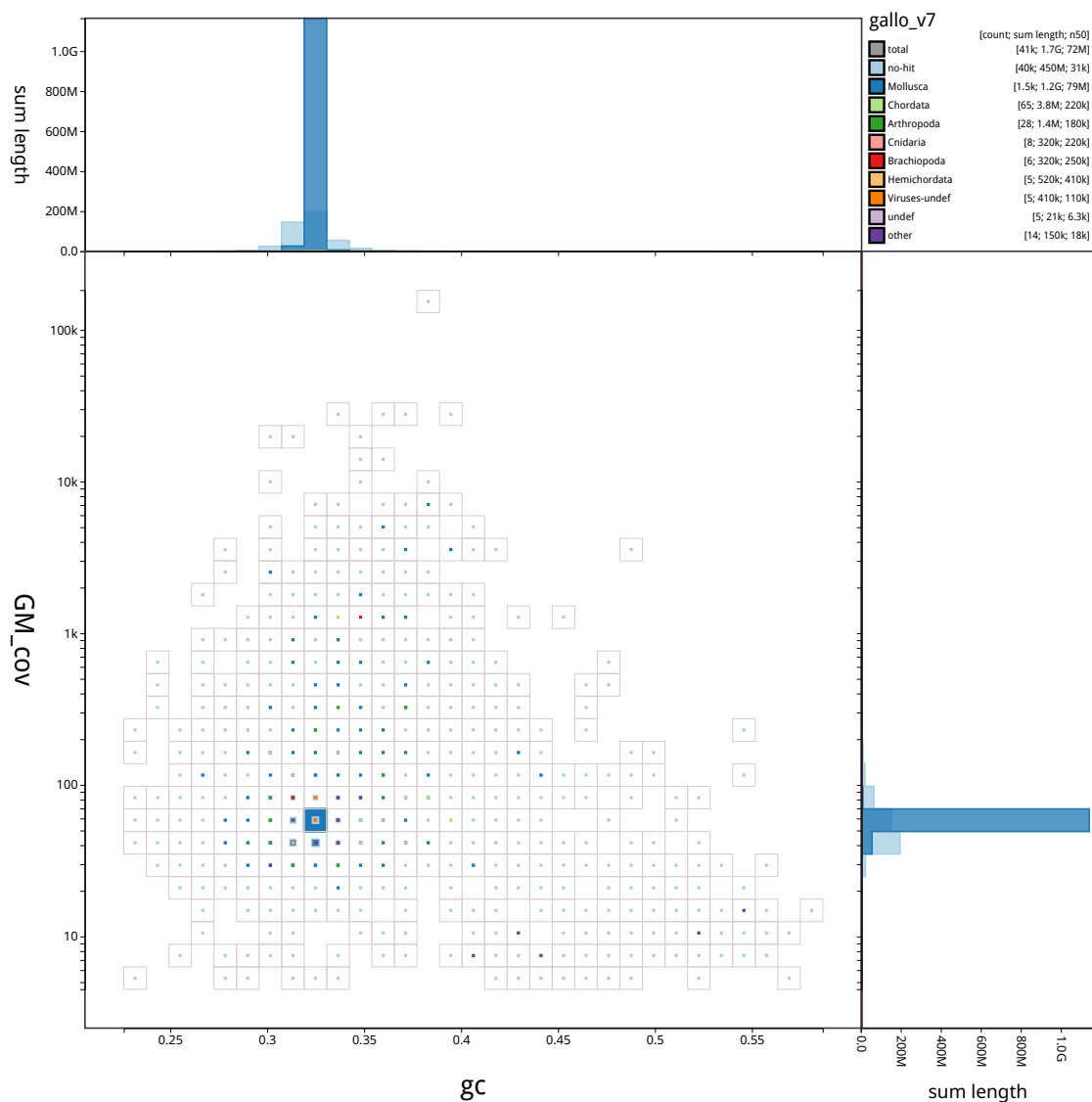


Figure S6: Blobtoolkit blob plot of base coverage in GM against GC proportion for scaffolds in assembly MgalMED_v7. Scaffolds are colored by phylum and binned at a resolution of 30 divisions on each axis. Colored squares within each bin are sized in proportion to the sum of individual scaffold lengths on a square-root scale, ranging from 1,005 to 1,127,105,406. Histograms show the distribution of scaffold length sum along each axis.

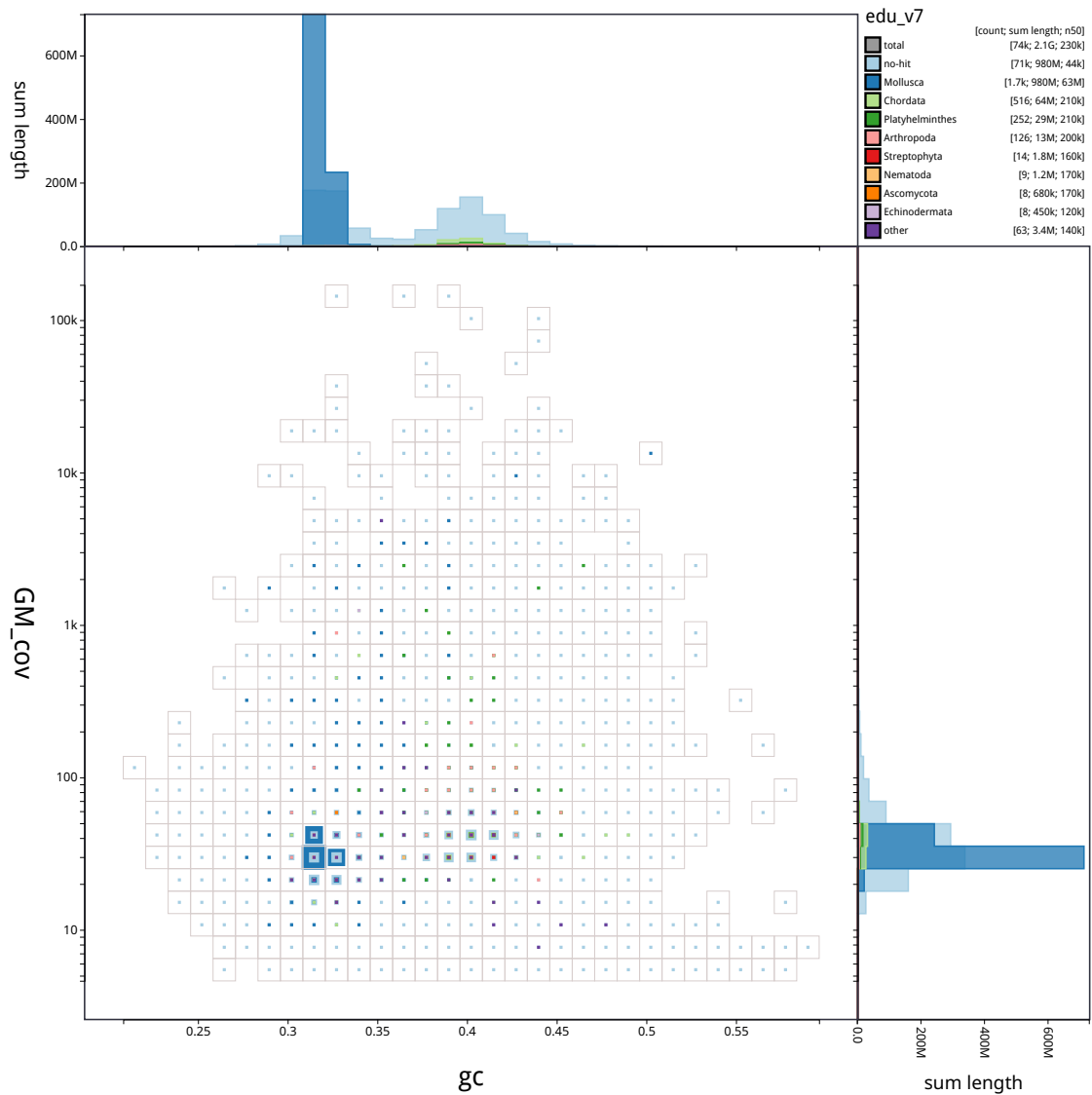


Figure S7: Blobtoolkit blob plot of base coverage in GM against GC proportion for scaffolds in assembly MeduEUS_v7. Scaffolds are colored by phylum and binned at a resolution of 30 divisions on each axis. Colored squares within each bin are sized in proportion to the sum of individual scaffold lengths on a square-root scale, ranging from 987 to 487,517,891. Histograms show the distribution of scaffold length sum along each axis.

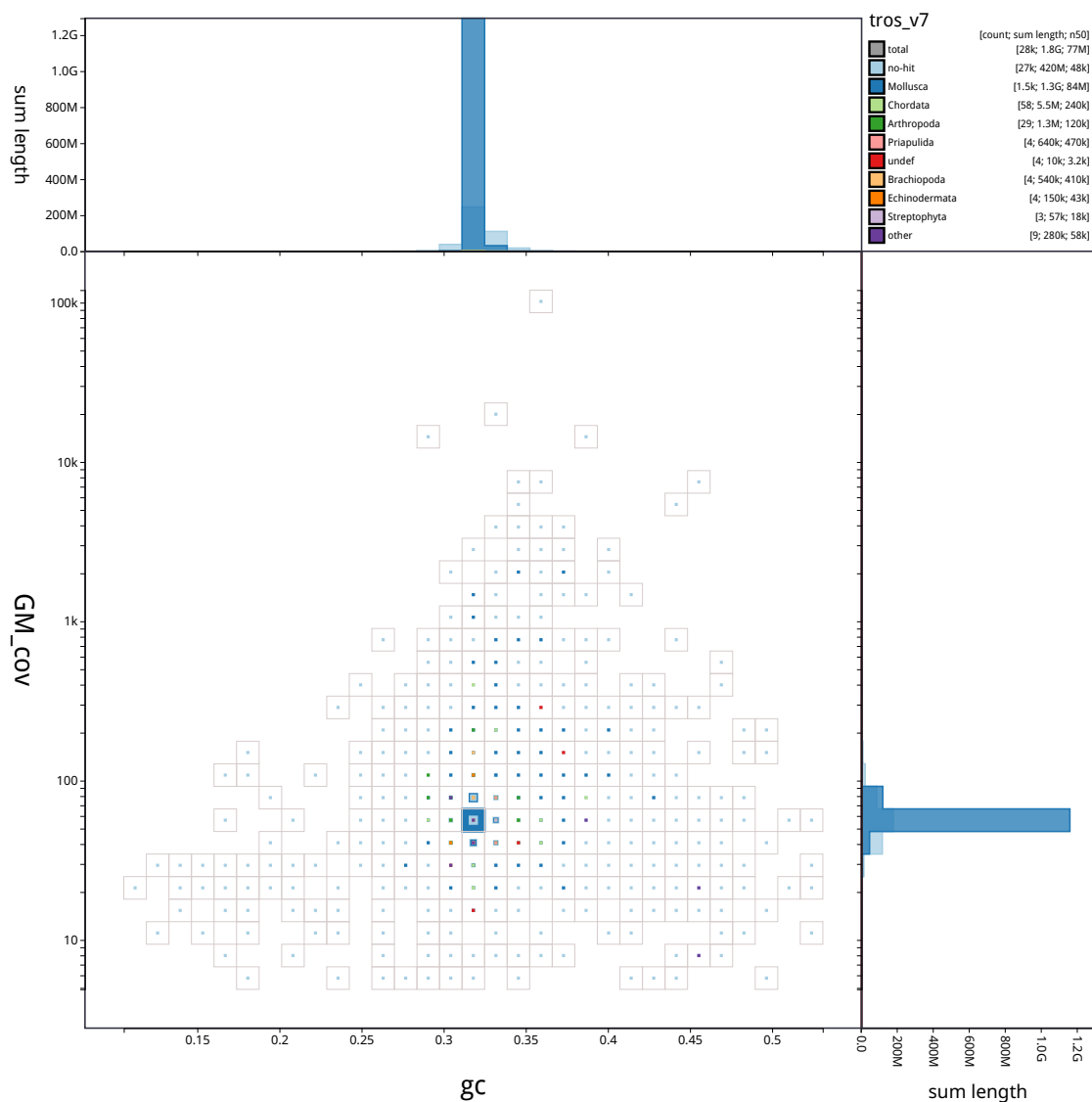


Figure S8: Blobtoolkit blob plot of base coverage in GM against GC proportion for scaffolds in assembly MeduEUN_v7. Scaffolds are colored by phylum and binned at a resolution of 30 divisions on each axis. Colored squares within each bin are sized in proportion to the sum of individual scaffold lengths on a square-root scale, ranging from 1,011 to 1,136,301,196. Histograms show the distribution of scaffold length sum along each axis.

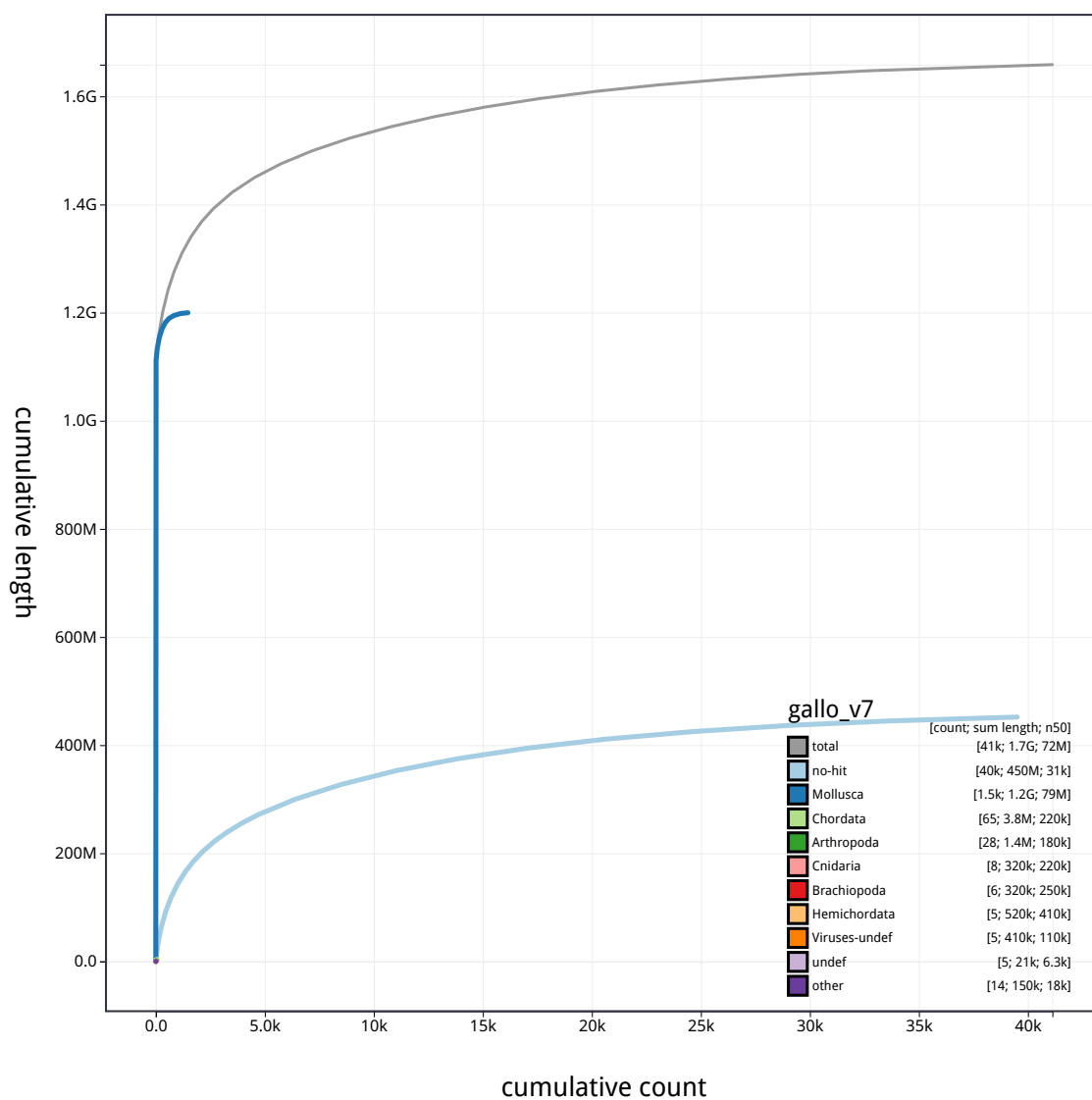


Figure S9: Blobtoolkit cumulative scaffold length for assembly MgalMED_v7. The gray line shows cumulative length for all scaffolds. Colored lines show cumulative lengths of scaffolds assigned to each phylum using the bestsumorder taxrule.

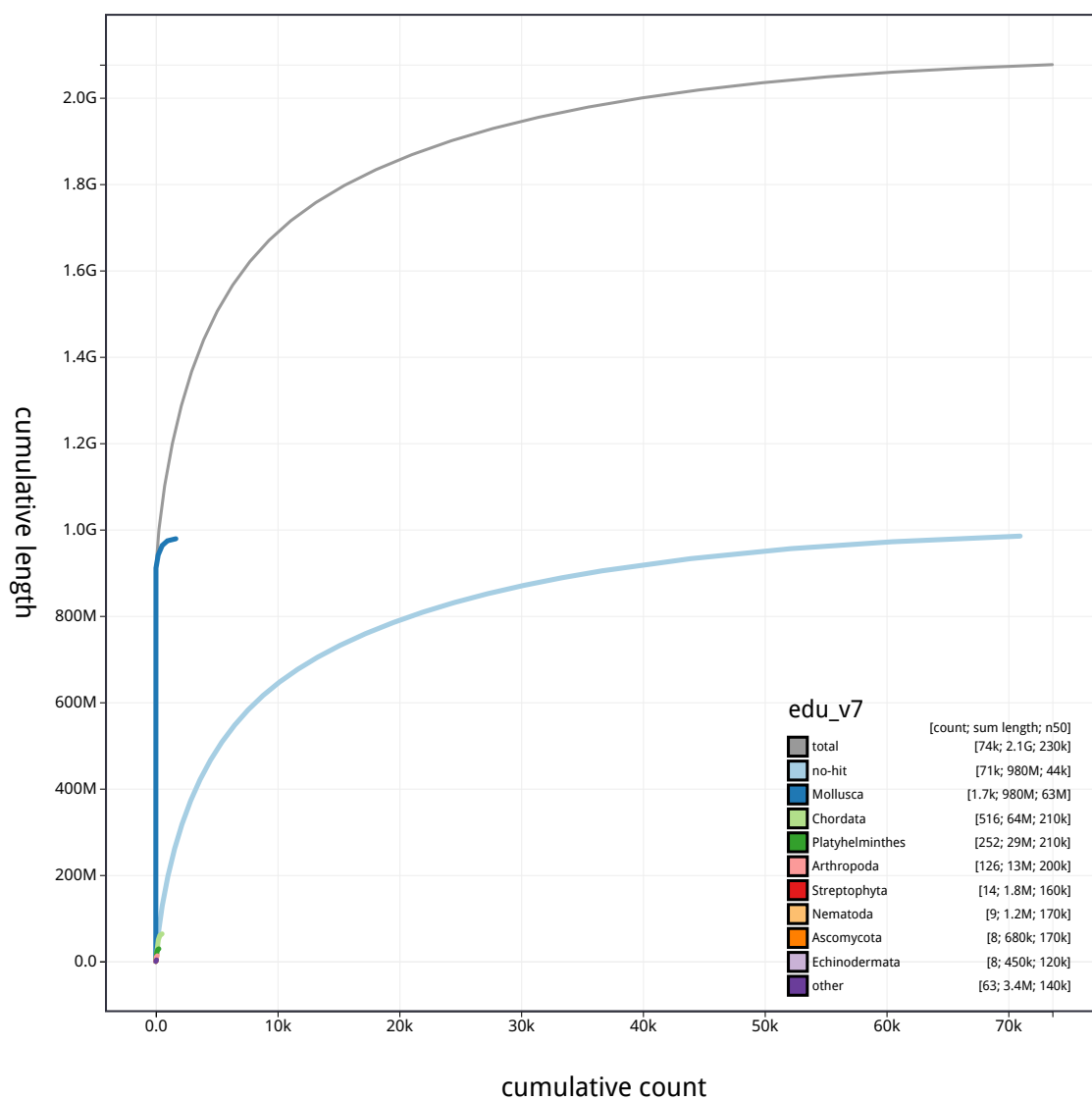


Figure S10: Blobtoolkit cumulative scaffold length for assembly MeduEUS_v7. The gray line shows cumulative length for all scaffolds. Colored lines show cumulative lengths of scaffolds assigned to each phylum using the bestsumorder taxrule.

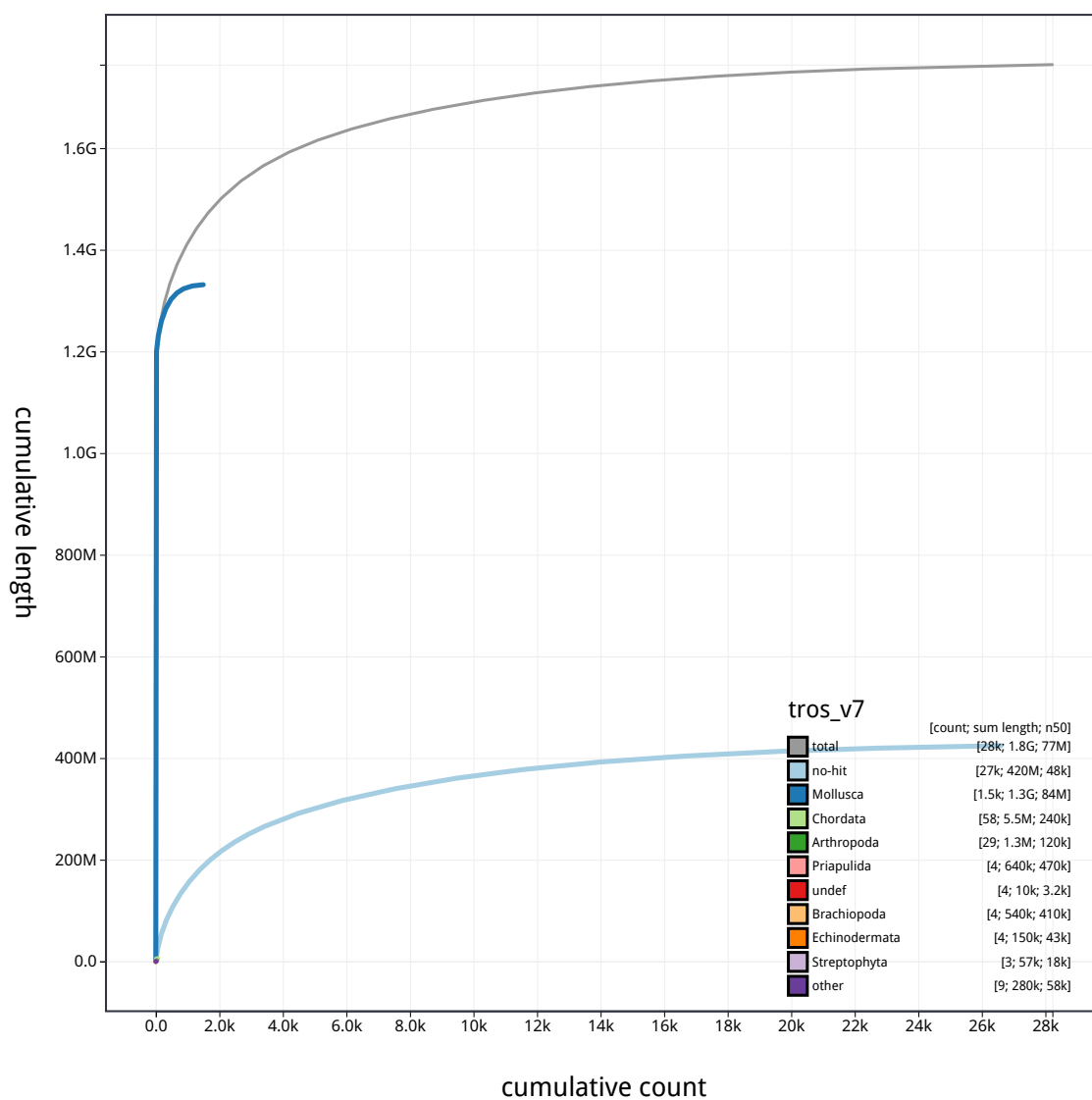











Figure S11: Blobtoolkit cumulative scaffold length for assembly MeduEUN_v7. The gray line shows cumulative length for all scaffolds. Colored lines show cumulative lengths of scaffolds assigned to each phylum using the bestsumorder taxrule.

Scaffold statistics

-  Log10 scaffold count (total 41k)
-  Scaffold length (total 1.7G)
-  Longest scaffold (100M)
-  N50 length (72M)
-  N90 length (16k)

BUSCO

mollusca_odb10 (5295)

-  Complete (74.0%)
-  Fragmented (6.5%)
-  Duplicated (6.0%)
-  Missing (19.4%)

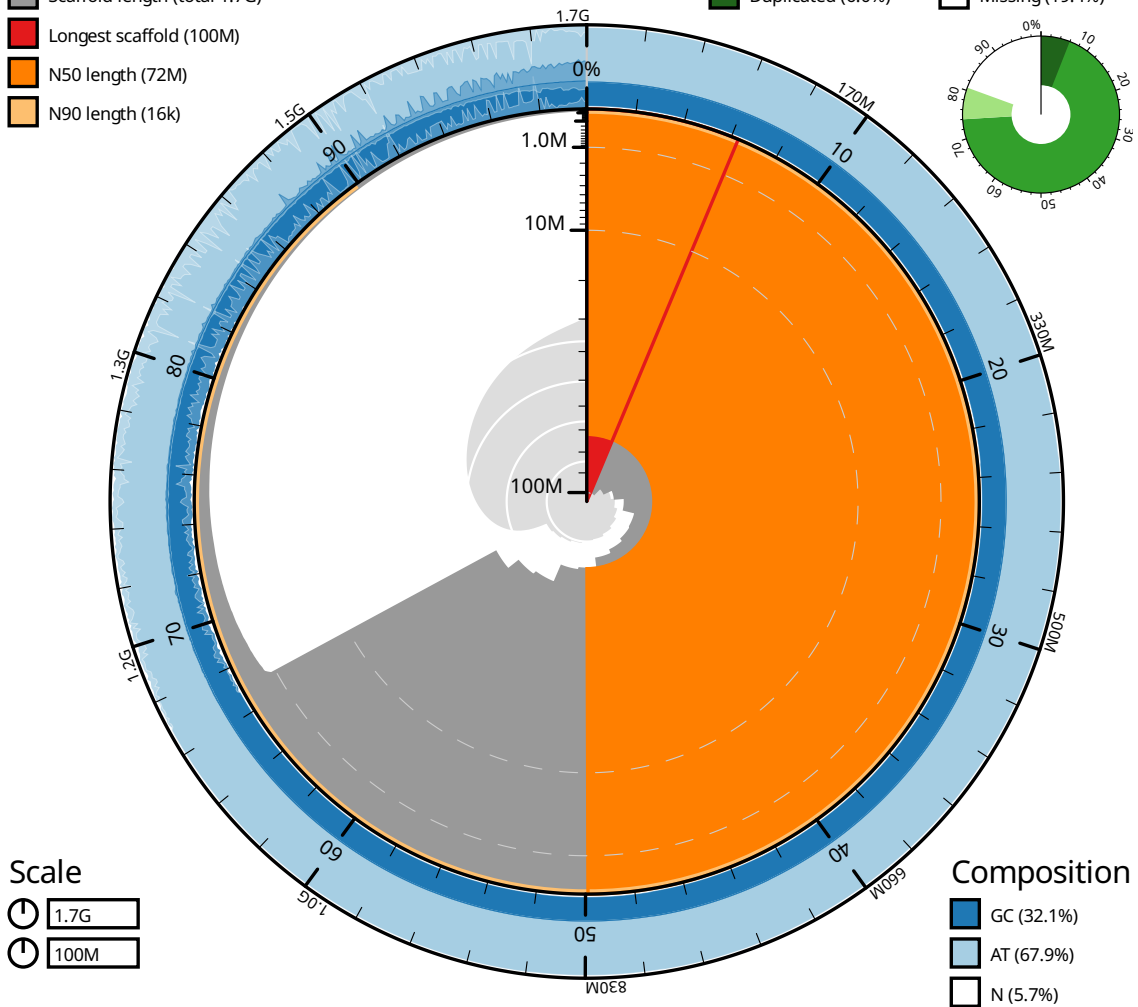











Figure S12: Blobtoolkit snail plot summary of assembly statistics for assembly MgalMED_v7. The main plot is divided into 1,000 size-ordered bins around the circumference with each bin representing 0.1% of the 1,658,656,017 bp assembly. The distribution of scaffold lengths is shown in dark gray with the plot radius scaled to the longest scaffold present in the assembly (104,729,878 bp, shown in red). Orange and pale-orange arcs show the N50 and N90 scaffold lengths (71,952,646 and 16,011 bp), respectively. The pale gray spiral shows the cumulative scaffold count on a log scale with white scale lines showing successive orders of magnitude. The blue and pale-blue area around the outside of the plot shows the distribution of GC, AT and N percentages in the same bins as the inner plot. A summary of complete, fragmented, duplicated and missing BUSCO genes in the mollusca_odb10 set is shown in the top right.

Scaffold statistics

-  Log10 scaffold count (total 74k)
-  Scaffold length (total 2.1G)
-  Longest scaffold (88M)
-  N50 length (230k)
-  N90 length (11k)

BUSCO

mollusca_odb10 (5295)

-  Complete (78.0%)
-  Fragmented (5.3%)
-  Duplicated (5.8%)
-  Missing (16.7%)

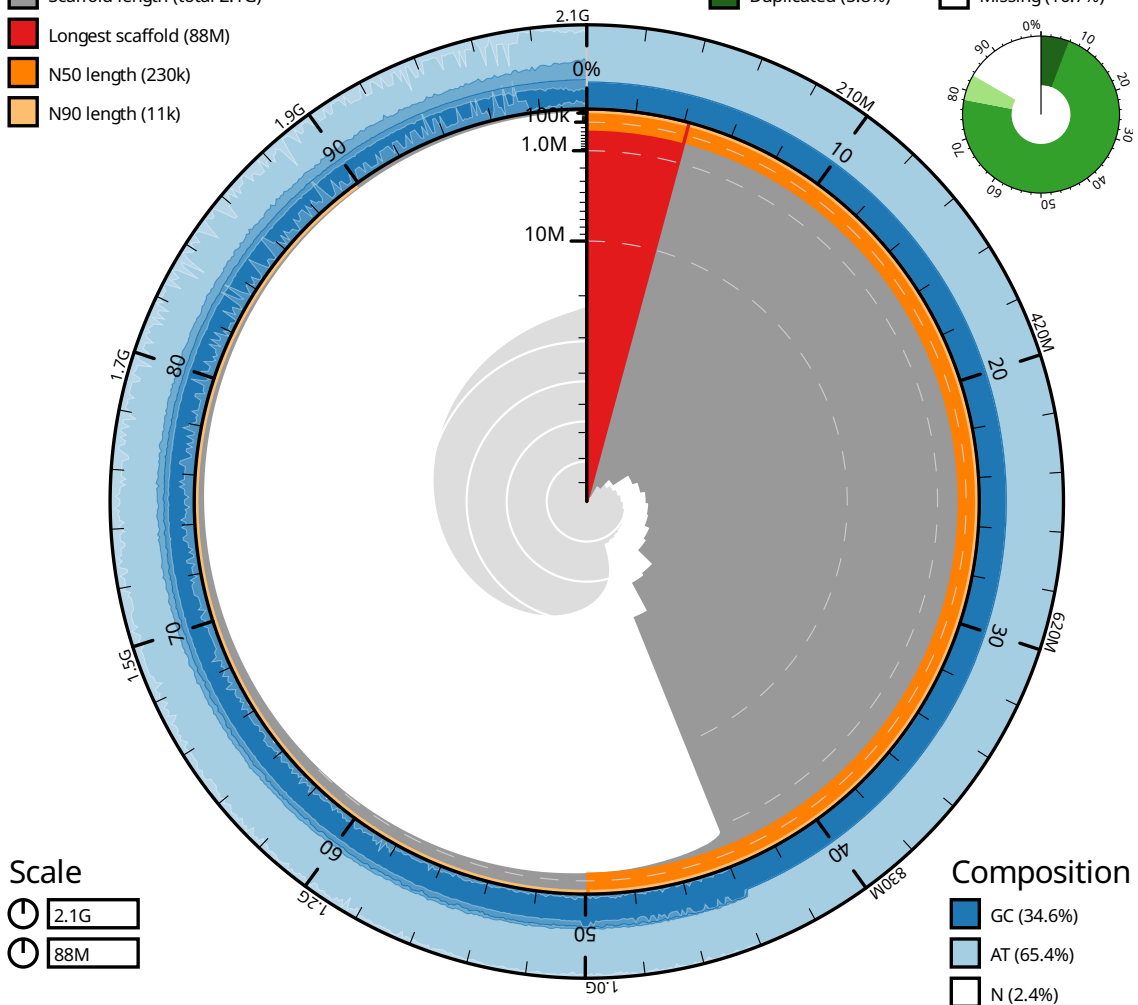


Figure S13: Blobtoolkit snail plot summary of assembly statistics for assembly MeduEUS.v7. The main plot is divided into 1,000 size-ordered bins around the circumference with each bin representing 0.1% of the 2,076,685,641 bp assembly. The distribution of scaffold lengths is shown in dark gray with the plot radius scaled to the longest scaffold present in the assembly (88,305,666 bp, shown in red). Orange and pale-orange arcs show the N50 and N90 scaffold lengths (228,263 and 10,773 bp), respectively. The pale gray spiral shows the cumulative scaffold count on a log scale with white scale lines showing successive orders of magnitude. The blue and pale-blue area around the outside of the plot shows the distribution of GC, AT and N percentages in the same bins as the inner plot. A summary of complete, fragmented, duplicated and missing BUSCO genes in the mollusca_odb10 set is shown in the top right.

Scaffold statistics

- Log10 scaffold count (total 28k)
- Scaffold length (total 1.8G)
- Longest scaffold (110M)
- N50 length (77M)
- N90 length (31k)

BUSCO

mollusca_odb10 (5295)

- Complete (76.3%)
- Fragmented (5.5%)
- Duplicated (10.0%)
- Missing (18.2%)

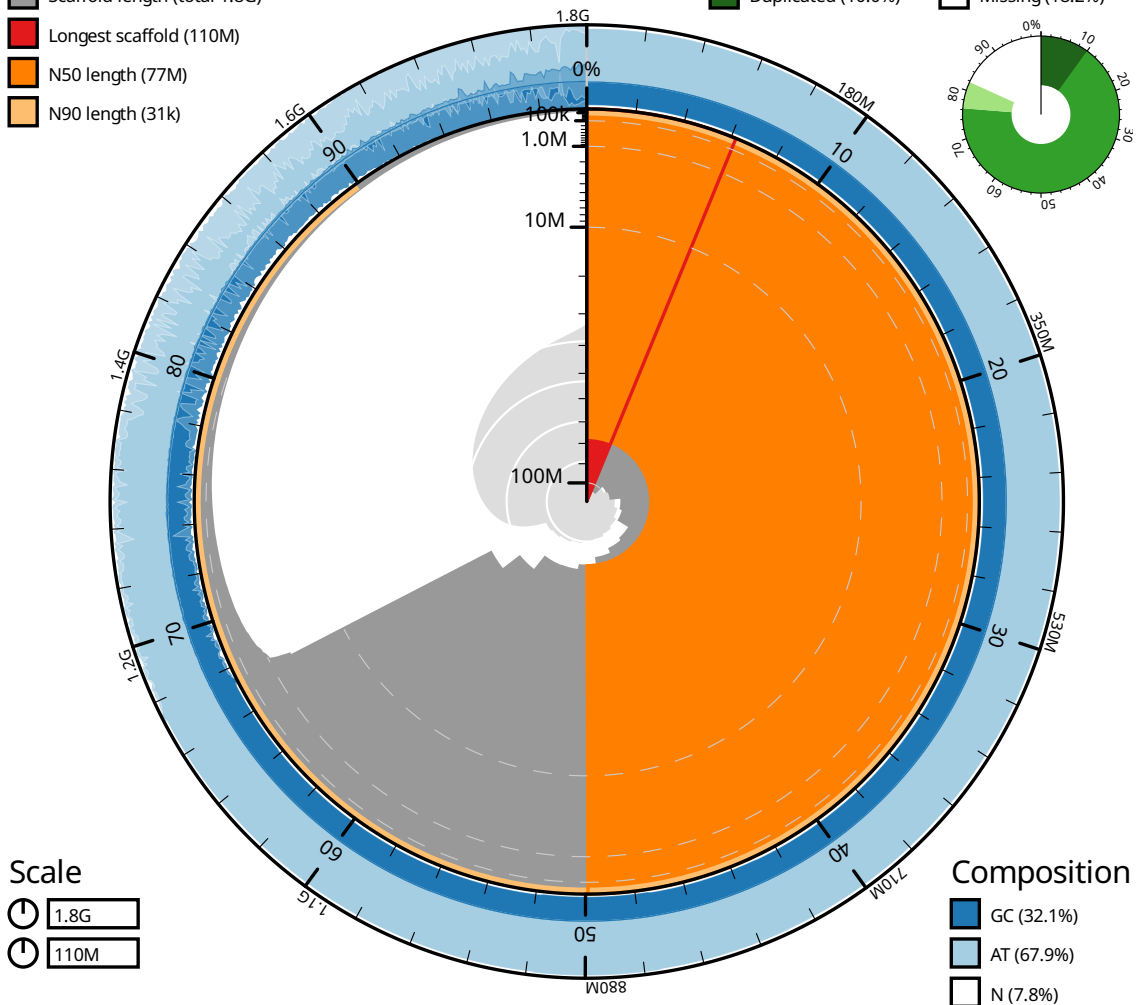


Figure S14: Blobtoolkit snail plot summary of assembly statistics for assembly MeduEUN_v7. The main plot is divided into 1,000 size-ordered bins around the circumference with each bin representing 0.1% of the 1,764,246,486 bp assembly. The distribution of scaffold lengths is shown in dark gray with the plot radius scaled to the longest scaffold present in the assembly (110,194,685 bp, shown in red). Orange and pale-orange arcs show the N50 and N90 scaffold lengths (77,102,752 and 30,649 bp), respectively. The pale gray spiral shows the cumulative scaffold count on a log scale with white scale lines showing successive orders of magnitude. The blue and pale-blue area around the outside of the plot shows the distribution of GC, AT and N percentages in the same bins as the inner plot. A summary of complete, fragmented, duplicated and missing BUSCO genes in the mollusca_odb10 set is shown in the top right.

Table S2: RepeatMasker results.

		MgalMED	MeduEUS	MeduEUN
Retroelements		17.89%	26.39%	17.91%
	SINEs:	0.03%	0.04%	0.03%
	Penelope	5.16%	5.31%	5.15%
	LINEs:	9.71%	13.83%	9.83%
	CRE/SLACS	0.00%	0.23%	0.00%
	L2/CR1/Rex	0.85%	3.86%	0.85%
	R1/LOA/Jockey	0.19%	0.14%	0.20%
	R2/R4/NeSL	0.04%	0.06%	0.04%
	RTE/Bov-B	1.60%	2.88%	1.66%
	L1/CIN4	0.57%	0.32%	0.53%
	LTR elements:	8.15%	12.52%	8.04%
	BEL/Pao	1.34%	3.18%	1.36%
	Ty1/Copia	0.08%	0.07%	0.09%
	Gypsy/DIRS1	3.37%	5.38%	3.34%
	Retroviral	0.01%	0.01%	0.01%
DNA transposons		2.09%	3.44%	2.06%
	hobo-Activator	0.18%	0.62%	0.18%
	Tc1-IS630-Pogo	0.19%	0.92%	0.18%
	En-Spm	0.00%	0.00%	0.00%
	MuDR-IS905	0.00%	0.00%	0.00%
	PiggyBac	0.02%	0.36%	0.03%
	Tourist/Harbinger	0.06%	0.04%	0.06%
	Other (Mi- rage, P-element, Transib)	0.00%	0.00%	0.00%
Rolling-circles		0.14%	0.10%	0.13%
Unclassified:		36.50%	30.64%	34.85%
Total interspersed repeats:		56.48%	60.47%	54.82%
Small RNA:		0.03%	0.09%	0.03%
Satellites:		0.04%	0.03%	0.04%
Simple repeats:		0.44%	0.35%	0.42%
Low complexity:		0.09%	0.07%	0.09%